

# BudgetFusion: Perceptually-Guided Adaptive Diffusion Models

Qinchuan (Wing) Li\* Kenneth Chen\* Changyue (Tina) Su Qi Sun

Tandon School of Engineering, New York University

{ql840, kc4906, cs7483, qisun}@nyu.edu



Figure 1. Given an input text prompt, our BudgetFusion model guides the number of denoising steps  $t$  before the generation starts. It balances the trade-off between visual perception quality and computational cost, achieving an optimized “quality gain per denoising step” efficiency.

## Abstract

Diffusion models have shown unprecedented success in the task of text-to-image generation. While these models are capable of generating high-quality and realistic images, the complexity of sequential denoising has raised societal concerns regarding high computational demands and energy consumption. In response, various efforts have been made to improve inference efficiency. However, most of the existing efforts have taken a fixed approach with neural network simplification or text prompt optimization.

Are the quality improvements from all denoising computations equally perceivable to humans? We observed that images from different text prompts may require different computational efforts given the desired content. The observation motivates us to present BudgetFusion, a novel model that suggests the most perceptually efficient number of diffusion steps before a diffusion model starts to generate an image. This is achieved by predicting multi-level perceptual metrics relative to diffusion steps. With the popular Stable Diffusion as an example, we conduct both numerical analyses and user studies. Our experiments show that BudgetFusion saves up to five seconds per prompt without compro-

mising perceptual similarity. We hope this work can initiate efforts toward answering a core question: how much do humans perceptually gain from images created by a generative model, per watt of energy?

## 1. Introduction

Diffusion models have been shown to produce images and videos of increasingly high fidelity [14]. However, this capability comes at the cost of significant computational demands due to the large number of inference steps required to generate images of high quality, which each require evaluation of large neural networks commonly having over 1 billion parameters [47]. The substantial computational burden of diffusion models has prohibited on-device deployment and led to societal concerns about their energy consumption and impact on the environment [18, 20, 49].

A significant body of recent literature has attempted to improve the efficiency of denoising diffusion models, such as reducing the number of denoising steps via neural network simplifications [23, 25] and model distillation [28, 37, 48, 50]. However, such one-size-fits-all approaches

\*The authors contribute equally to this paper.

inevitably lead to images generated with inconsistent quality depending on the desired content reflected in the text prompts. For example, consider the two prompts: 1) “a white and empty wall” vs. 2) “a colorful park with a crowd” as shown in Figure 2. Intuitively, the two prompts may require different number of inference steps to generate images of high quality. With this inspiration, we present BudgetFusion, a perceptually-aware guidance model for text-to-image diffusion models. Specifically, for a given text prompt, BudgetFusion estimates the correlation between various visual quality metrics and number of diffusion inference steps as a time series function. The estimation then suggests the optimal number of denoising steps with a gradient-based analysis. That is, we determine the plateau point where additional denoising steps will benefit only marginally in terms of visual perception. To achieve this goal, we first created a large-scale generative dataset using more than 18,000 text prompts  $\times$  12 timesteps. By leveraging this data, we can measure perceptual similarity at various scales, ranging from per-pixel errors to spatial layout and semantics. From this perceptual assessment of generative images and the Markov Chain nature of diffusion models, we developed a long short-term memory (LSTM) neural network [11] that predicts the relationship between quality enhancement and diffusion steps.

We conduct a series of objective analyses and subjective user studies. Our findings demonstrate BudgetFusion’s effectiveness in significantly enhancing the computational efficiency of diffusion models, measured as perceptual gain per diffusion step. Moreover, this enhancement is achieved without compromising subjectively perceived quality. We hope this work will spark a series of future initiatives on human-perception-centered approaches for computation- and energy-friendly generative models<sup>1</sup>.

## 2. Related Work

### 2.1. Optimizing Generative Diffusion Models

Diffusion models have recently exploded in popularity due to their high performance on tasks such as image and video generation, audio generation, and 3D shape generation [14, 46]. Latent diffusion models [47] have significantly improved training and inference efficiency, but still require a high number of forward denoising neural network evaluations to produce high-quality results. To tackle this problem, an extensive body of literature has been proposed to optimize and accelerate diffusion models from different perspectives. For example, optimizing the sampling strategy may enable more efficient denoising computation [2, 23, 25], such as timestep integration [40] or conditioning on the denoising [44]. Additionally, by approximating the direct mapping from the initial noise to generated im-

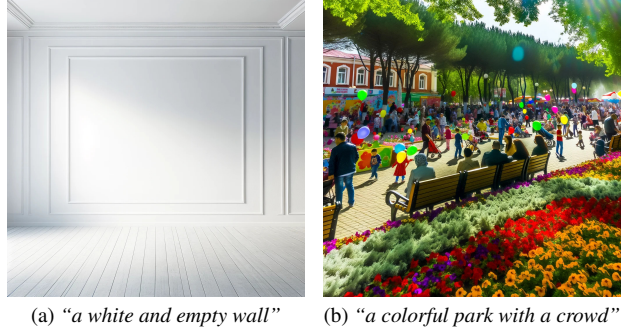


Figure 2. *Example generative images with different visual complexity.* With current diffusion models, the two images are generated with the same denoising steps and computational cost. However, intuitively, the simpler (a) could have been generated with less computation than (b). This insight motivates us to develop BudgetFusion, an efficiency-optimized guidance for balancing quality vs. computation trade-offs. BudgetFusion tailors the denoising process to align with the given prompt before generation starts.

ages [30, 53], denoising can be executed with a reduced number of steps. After the models are pre-trained, distilling them to student models can generate specific images with fewer steps [28, 37, 48, 50]. Optimized solvers for the denoising step can efficiently reduce the computation to avoid re-training or fine-tuning [19, 27, 29, 52].

While reduced computation often results in degraded image quality, existing approaches typically prioritize computational models over human perception. For instance, as shown in Figure 2, different text prompts could be allocated with varying levels of computation to achieve similar visual quality from a human perspective. To our knowledge, the perceptual correlation between prompt-indicated visual content complexity and computational cost remains unknown and is not yet integrated into the diffusion model workflow. In this research, our BudgetFusion introduces the first complementary human perception-aware approach, guiding diffusion computation toward the most efficient “perceived quality gain per step” tailored to the prompt.

### 2.2. Perceptually-Guided Computer Graphics

A wealth of literature in the graphics community has studied applications of human perceptual data to optimize visually-based algorithms. For example, several image quality metrics have been proposed which generally agree with experimental data, such as SSIM [56] or PSNR, or neural network-based metrics like LPIPS [60]. Metrics which are based on psychophysical models are more highly correlated with human responses, and can model temporal, high luminance, and foveated artifacts [7, 33, 35]. Recently, metrics such as DreamSim [9] have been proposed to determine higher-order image differences, such as layout or seman-

<sup>1</sup>We will release the code and data upon acceptance.

tics. Several techniques are built with human perception in mind, such as for optimizing traditional rendering pipelines [16, 43] or for improving the performance of generative models [6, 17]. However, there has been little investigation into understanding and optimizing generative content from the perspective of perceptual guidance.

### 3. Method

We develop BudgetFusion to suggest the optimal number of inference, or denoising, steps based on predicted perceptual quality. Toward this aim, and as visualized in Figure 3, we first created a dataset of images generated with different numbers of denoising steps (Section 3.1). To comprehensively measure the perceptual quality of this large-scale synthetic dataset, we leveraged perceptual metrics at various levels of detail, including their pixel-wise error, layout, and overall semantic similarity with respect to "reference" images generated with a large number of inference steps (Section 3.2). With the jointly labelled data of text prompt, perceptual scores, and denoising steps, we train an LSTM-based BudgetFusion model to predict metric scores against denoising steps as a time series function, given input prompts (Section 3.3). Lastly, we employ BudgetFusion to estimate the least required number of denoising steps which produces high-quality images using plateau point estimation (Section 3.4).

#### 3.1. Synthetic Dataset Generation

We first generated an image dataset by running the forward pass of a diffusion model at different number of denoising steps in order to understand the change in perceptual quality throughout timesteps. To this end, we sample a large set of text prompts and denoising steps to be used to generate images with a diffusion model.

We used the popular pre-trained Stable Diffusion 2 model (SD)<sup>2</sup>, a variant of Stable Diffusion [47], as a drop-in to demonstrate BudgetFusion. Stable Diffusion 2 generates high-quality images despite faster inference time compared to larger models, like Diffusion XL. Note that BudgetFusion may be applied to other diffusion model architectures without loss of generality.

**Creating and sampling prompts.** To obtain prompts that cover a wide range of semantics from real-world scenarios, we use an existing image-caption pair dataset, COCO [26]. However, the dataset contains more than 330,000 images, making it computationally infeasible to generate a corresponding image for each of the captions as a prompt using diffusion models. Therefore, we systematically sample the most representative captions using the Cosine dissimilarity score  $C_{clip}$  in the CLIP-encoded space [45], where higher

$C_{clip}$  indicates more similar text pairs. That is, to construct the prompt set  $\mathbf{P}$ , we keep the prompts so that their pairwise CLIP similarity is lower than a threshold

$$S(p, p') < \hat{S}, \forall p, p' \in \mathbf{P}. \quad (1)$$

We experimentally set the value of  $\hat{S}$  to .75, and acquired 18,384 prompts to compose  $\mathbf{P}$ . The sampled text prompts are then used to generate images at different denoising steps using SD.

**Sampling denoising timesteps.** In most existing diffusion models, the computation could be reduced by skipping denoising timesteps with the cost of reduced quality. Therefore, the main aim of BudgetFusion is to suggest the most efficient trade-off between perceptual quality and computation cost based on a specific text prompt. Toward this aim, for all text prompts in  $\mathbf{P}$  we generate images at various denoising steps to make a systematic measurement of the change in image quality at each step, as shown in Figure 3b. Because it is computationally infeasible to perform image generation for all possible timesteps, we consider a power law as guidance to sample the diffusion timestep set  $\mathbf{T} := \{t_1, \dots, t_N\}$ . Specifically, we select  $t_i = 1 + 2^{i-1}$ , and additionally include a boundary timestep  $\{t_1 = 1\}$  and empirically sample intermediate conditions,  $\{22, 27, 42\}$ , to further increase the sampling density. We sample this range up to 129 ( $i = 8$ ), which is above the commonly accepted sufficient range of 100 inference steps for Stable Diffusion [39]. This sampling strategy results in  $N = 12$  time steps in total.

**Scheduler and generation.** All the experiments in our work use the widely used Euler Scheduler [19]. We make this choice due to the scheduler’s more consistent and cohesive evaluation results because of its fixed start (1) and end (1000) timesteps. We have 4 fixed random seeds as the generator of the initial noise and PyTorch manual random seeds that control the stochastic denoising process. Using the sampled conditions, we generate an image  $I_{p,t}$  from each of the selected prompts in  $\mathbf{P}$  at each representative time step in  $\mathbf{T}$  and 4 random seeds using SD. Overall, the dataset contains  $18,384 (p) \times 12 (N) \times 4(\text{seeds}) = 882,432$  images of resolution  $768 \times 768$ . We reserved the images from 90% of randomly sampled prompts as the training set (Section 3.3) and the remaining 10% for evaluation (Section 4).

#### 3.2. Multi-Scale Perceptual Metrics

We measure the perceptual quality throughout the synthetic dataset of an image  $I$  corresponding to prompt  $p$  and timestep  $t$ , denoted as  $\{I_{p,t}\}$ . The denoising process over  $t$  iteratively removes noise to generate the final image. Each step jointly enhances local details and/or global image-text

<sup>2</sup><https://github.com/Stability-AI/stablediffusion>



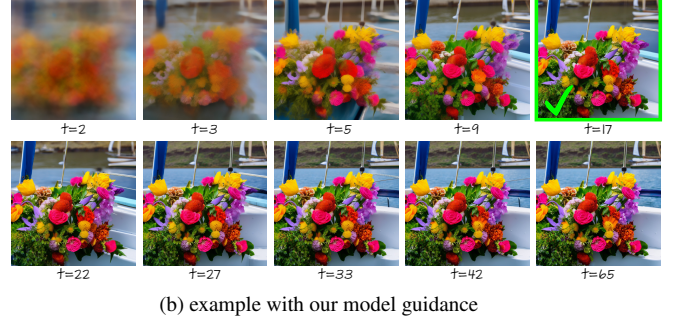
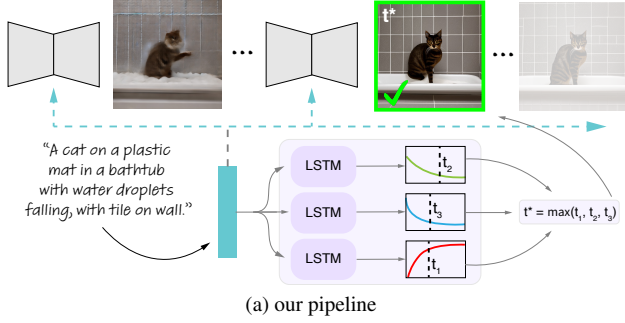


Figure 3. *Our BudgetFusion pipeline.* (a) Given an input prompt, we predict three time series of perceptual quality metrics of the generated images at different timesteps (the three colored curves). Each one of them represents a given perceptual scale. The model determines the optimal timestep,  $t^*$ , which is the max plateau point of the three metrics, described in Sec. 3.2. The pre-trained diffusion model performs  $t^*$  number of denoising steps, rather than continuing the forward process, which would only yield little image quality improvement as predicted by our model. (b) We include an additional example of the forward process and the selection made by our model.

alignment [58]. Therefore, image quality should be measured at various perceptual scales in terms of level of detail and semantics. To this end, we propose to leverage three perceptual metrics to compare images generated at each step. First, we measure the most detailed pixel-level quality using Laplacian signal-to-noise ratio (L-SNR) [21]. Then, we leverage the recent learning-based layout-aware DreamSim metric (D-SIM) [9] to measure mid-level content similarity. Lastly, we measure the high-level semantic alignment using the Cosine similarity in CLIP-encoded latent space (I-CLIP) [45]. Both D-SIM and I-CLIP metrics compare each image  $I_{p,t}$  against the target image ( $I_{p,t_N}$ ,  $t_N = 129$ ).

**Pixel-level: Laplacian signal-to-noise ratio (L-SNR  $\in [0, 1]$   $\downarrow$ )** An insufficient number of forward denoising steps may generate noisy and distorted images [58]. Therefore, we first measure each image’s pixel-level quality. The signal-to-noise ratio (SNR) is a widely adopted metric for image quality [21] and deep metric learning [59]. To our aim, we employ the SNR as a no-reference L-SNR metric, which assesses the SNR by comparing the original image to its Laplacian-filtered version, thereby evaluating its sharpness [42].

$$\text{L-SNR}(p, t) := \text{SNR}(I_{p,t}, G \circledast I_{p,t}), \quad (2)$$

where  $G$  and  $\circledast$  are the Gaussian kernel ( $\sigma = 1$ ) and convolution operator, respectively. We developed this measurement instead of using reference-based image quality metrics (e.g., PSNR) against the target image  $I_{p,t_N}$  due to the stochastic and random nature of diffusion model-based generation, where pixel-level values can significantly vary based on the added random noise.

**Mid-level: DreamSim (D-SIM  $\in [0, 1]$   $\downarrow$ )** The DreamSim metric was recently proposed by Fu et al. [9]. It mea-

sures mid-level perceptual similarity between two images, considering non-pixel factors such as spatial layouts. We compute the D-SIM metric as

$$\text{D-SIM}(p, t) := D_s(I_{p,t}, I_{p,t_N}), \quad (3)$$

where  $D_s$  indicates the DreamSim distance.

**Semantic-level: image caption encoded by CLIP (I-CLIP  $\in [0, 1]$   $\uparrow$ )** The CLIP model [45] maps text and image embeddings into the same latent space, and has been used for image captioning [1, 26] and other text-conditional generation tasks, such as image generation [47, 57], and 3D mesh generation [38]. On the highest level, a poorly generated image may semantically mis-align with an input prompt [58]. Therefore, determining the captions between a pair of images may reflect their contextual and semantic distances. With this observation in mind, we generate the CLIP-encoded caption for each image, and compare their distance in the encoding space,

$$\text{I-CLIP}(p, t) := \cos(\overline{C}(I_{p,t}), \overline{C}(I_{p,t_N})), \quad (4)$$

where  $C$  is CLIP captioning, and  $\overline{C}$  is the latent embedding.

### 3.3. Learning to Predict Perceptual Metrics from Text

The multi-scale perceptual analysis of each image  $I_{p,t}$  creates a large-scale dataset of prompt - timestep pairs which map to the three metrics scores computed on images generated at the corresponding timestep by averaging all scores over the four random seeds,

$$(p, t) \rightarrow \{\text{L-SNR}(p, t), \text{D-SIM}(p, t), \text{I-CLIP}(p, t)\}. \quad (5)$$

For each prompt  $p$ , the per-time step data informs the perceptual quality at a given denoising timestep  $t$ . We



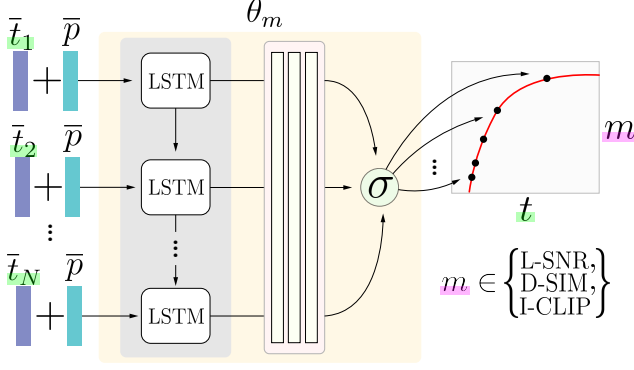


Figure 4. *Model architecture.* We visualize our architecture as an unrolled LSTM,  $\theta_m$ , which takes as input positionally-embedded timestep,  $\bar{t}_i$ , and clip-embedded prompt,  $\bar{p}$ . Outputs for each timestep are fed to fully-connected layers, and normalized with a sigmoid activation to produce scores,  $m$ , which are one of three perceptual metrics defined in Section 3.2.

then trained neural networks  $\theta_m$  to predict each of the above time series for novel text prompts. Here,  $m \in \{\text{L-SNR}, \text{D-SIM}, \text{I-CLIP}\}$  are the individual perceptual metrics.

**Model architecture** To simulate the change in image quality with respect to the number of denoising steps, the model architecture should reflect the locally dependent chain nature of the denoising process of diffusion models. With this insight, we choose to use a bidirectional LSTM (BiLSTM) [10] given the robustness and accuracy observed for various similar time series prediction tasks [51]. Our model architecture is visualized in Figure 4. To transfer the stochastic chain process to a recurrent form for the LSTM, the CLIP-embedded text prompt  $\bar{p}$  and positionally-embedded (as in Kenton and Toutanova [22]) timestep  $\bar{t}$  vectors are combined as input to predict metric scores at timestep  $t$ ,

$$m_t(p) = \theta_m(\bar{p} + \bar{t}). \quad (6)$$

The implementation details of our model are discussed below.

**Model implementation details** As shown in Figure 4 and similar to prior literature [3, 32, 41, 54], we implement  $\theta_m$  as a simple BiLSTM, followed by a feed-forward fully connected network (MLP) and Sigmoid activation. Specifically, for the LSTM, we use a two-layer BiLSTM with hidden features of size 512. The three-layer MLP transforms the LSTM-returned hidden scores of size 1024 (due to the bidirectional design) to 128 and then 1. We train the model with our held-out 90% (Section 3.1) training images from 16,545 prompts with L2 loss, a batch size of 32, and a learning rate of 1e-4. During training, we used the widely

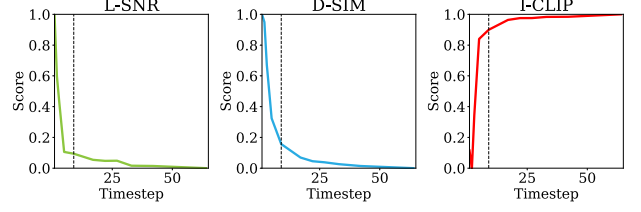


Figure 5. *Example results of predicting denoising steps before generation.* By leveraging predicted perceptual metrics with regard to timesteps as a time series, we predict the “plateau points” for each. Their max (Equation (7)) suggests the most efficient timesteps for diffusion models, before the generation starts.

adopted DropOut [13] technique on the output of the bidirectional LSTM. To enhance the fitting ability of the model, we linearly interpolate the scores from sampled steps in  $\mathbf{T}$  to get pseudo-ground-truth scores for all other steps. Finally, we train our model for L-SNR and D-SIM with 25 epochs and for I-CLIP with 50 epochs.

### 3.4. Predicting Denoising Steps from Perceptual Metrics

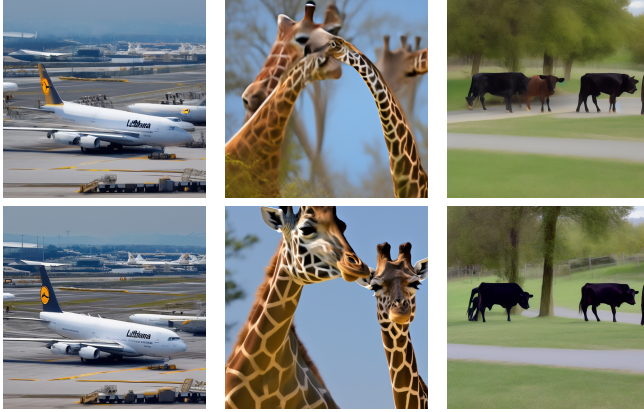
For a new prompt  $p$ , we leverage the trained LSTM models  $\theta_m$  to predict the time series  $m_t$  for each  $m \in \{\text{L-SNR}, \text{D-SIM}, \text{I-CLIP}\}$ . Our goal is to suggest the total denoising timestep of the diffusion models before generation. As shown in Figure 5, we intuitively find the “turning” timestep  $t^*$  where all metrics plateau. That is, additional inference steps ( $t > t^*$ ) will only improve users’ perceived image quality marginally at all scales, indicating reduced computational efficiency. Note that the perceptual metrics typically exhibit a monotonic relationship with regard to number of denoising timesteps, i.e., larger timesteps do not reduce the perceived quality. Inspired by prior literature on turning point detection for psychological time series data [8], we employ a statistical approach to determine optimal time step,

$$\begin{aligned} t^*(p) &:= \max_t t_m^*(p), \quad m \in \{\text{L-SNR}, \text{D-SIM}, \text{I-CLIP}\} \\ t_m^*(p) &:= \max_t \text{ s.t. } m_t(p) \geq \mu(\{m_t(p)\}_{t=t_1}^{t_N}) + \omega_m \sigma(\{m_t(p)\}_{t=t_1}^{t_N}). \end{aligned} \quad (7)$$

Here,  $\mu(\cdot)/\sigma(\cdot)$  indicates the median and standard deviation of the time series data. Similar to Engbert and Mergenthaler [8], we determine the weights  $\omega_m$  ( $\omega_{\text{L-SNR}} = 0.3, \omega_{\text{D-SIM}} = 0.2, \omega_{\text{I-CLIP}} = 0.5$ ) of the three metrics using the efficiency measurement as detailed in Section 4.2. The effectiveness of the suggested step numbers on each perceptual metrics is visualized in Figure 6.

## 4. Evaluation

Beyond the qualitative results demonstrated in Figure 7 and the supplementary material, we first evaluate the model



(d) BudgetFusion L-SNR (e) BudgetFusion D-SIM (f) BudgetFusion I-CLIP

Figure 6. *Sufficiency of BudgetFusion-suggested denoising steps.* The first/second row visualizes example images with step numbers below/from our model suggestion. Each column compares the effectiveness of corresponding perceptual metrics. (a) vs. (d): insufficient denoising steps caused blurry image, reflected as low L-SNR values. (b) vs. (e): insufficient denoising steps caused structural and geometric distortion, reflected as low D-SIM values. (c) vs. (f): images generated from text prompt “black cows following on another across the street[...]”. Insufficient denoising introduces brown cows that are semantically undesired from the prompt.

prediction accuracy as an ablation study in Section 4.1. Then, we measure BudgetFusion’s effectiveness in enhancing computational efficiency as “perceptual gain per diffusion step” Section 4.2, as well as the generated content diversity Section 4.3. Lastly, we conduct an user study for subjective measurement of overall generated image quality Section 4.4. To this aim, we study and compare three conditions:

- **OURS**: Our adaptive BudgetFusion method;
- **UNIFORM**: Instead of adaptive guidance, we construct a baseline which suggests a single timestep for all prompts. By calculating the average step numbers from BudgetFusion throughout the evaluation set, this condition achieves, on average, the same computation cost to **OURS**;
- **REFERENCE**: Within our sampled timesteps  $\mathbf{T}$ , we select  $t = 65$ , which is close to the commonly and empirically suggested number of denoising steps. Higher step sizes will only marginally enhance quality.

In the following experiment, we use the holdout test set of 1,839 prompts, which is 10% of the entire image dataset.

#### 4.1. Ablation Study: Model Prediction Accuracy

We evaluate our design of the proposed text-to-metric time series LSTM model (Section 3.3) as an ablation study. We computed mean absolute error (MAE, lower is better) between the predicted and measured ground truth to measure



Figure 7. *Qualitative results.* We display two additional examples which show visible differences between subsequent timesteps. The middle column in each row represents the images generated by the optimal timestep suggested by our model. Their quality differences from the previous timestep (left) are large, but small from the next timestep (right). See supplementary material for more cases.

Table 1. Ablation study of model MAE loss ( $\downarrow$ ) for the perceptual metrics described in Sec. 3.2.

Model	$ \Delta\text{L-SNR} $	$ \Delta\text{D-SIM} $	$ \Delta\text{I-CLIP} $
<b>OURS</b>	<b>.026</b>	<b>.037</b>	<b>.031</b>
<b>OURS</b> w/o t-encoding $\bar{t}$	.059	.239	.134
MLP+Tanh replacing LSTM	.068	.241	.137

prediction accuracy. Specifically, we compare the MAE of **OURS**, and **OURS** without text embedding (to validate the choice of embedding), as well as replacing our LSTM model with MLP + Tanh activation (to validate the choice of using LSTM). Table 1 shows the results of our ablation. **OURS** exhibits significantly lower error among all alternative design choices. The results evidence the effectiveness of the text prompt encoding and LSTM neural network.

#### 4.2. Quality and Computational Efficiency

The ultimate goal of BudgetFusion is to optimize the “quality gain per watt of computation” of diffusion models. Therefore, we evaluate its quality versus its computation efficiency against the aforementioned conditions.

**Quality-Computation Efficiency** We measure quality-computation efficiency as the perceptual quality gain per TFLOPS computation in the GPU. That is, for each evaluation prompt  $p$  and metric  $m$ , we compute

$$\frac{m_t(p)}{\eta}. \quad (8)$$

Table 2. Quality-computation efficiency ( $\uparrow$ ) per step mean and standard error for different metrics and conditions (e-2 scaled). As raw L-SNR and D-SIM values are negatively correlated to the quality, we inverted them here for consistency.

Model	(1-L-SNR) / $\eta$	(1-D-SIM) / $\eta$	I-CLIP / $\eta$
<b>OURS</b>	<b>0.46</b> $\pm$ 1.3e-2	<b>1.38</b> $\pm$ 1.1e-2	<b>1.48</b> $\pm$ 1.2e-2
<b>UNIFORM</b>	0.42 $\pm$ 2.0e-3	1.28 $\pm$ 1.8e-3	1.36 $\pm$ 1.7e-3
<b>REFERENCE</b>	0.25	0.25	0.25
DDIM [52]	0.41 $\pm$ 2.1e-3	1.17 $\pm$ 2.5e-3	1.32 $\pm$ 2.0e-3
DeepCache [31]	0.43 $\pm$ 2.0e-3	1.27 $\pm$ 1.8e-3	1.35 $\pm$ 1.7e-3
DistriFusion [24]	0.44 $\pm$ 2.1e-3	0.87 $\pm$ 3.1e-3	1.22 $\pm$ 2.6e-3
EulerAncestral	0.38 $\pm$ 1.8e-3	1.0 $\pm$ 2.6e-3	1.26 $\pm$ 2.4e-3

Here,  $\eta$  denotes the overall computation cost approximated as the TFLOPs (FLoating-point OPERations) during model inference. Higher average values indicate greater efficiency in quality gain. Beyond the three conditions **OURS** ( $\eta \approx 68$  T), **UNIFORM** ( $\eta \approx 67$  T), and **REFERENCE** ( $\eta \approx 394$  T), we further compared with alternative approaches in the literature on efficient diffusion models. In particular, we compared with the original denoising diffusion implicit models (DDIM) [52], DeepCache [31], DistriFusion [24], as well as adding ancestral sampling with Euler method steps (EulerAncestral). For fair comparison in computing the efficiency metrics, these approaches were controlled to consume the TFLOPs between **UNIFORM** and **OURS**, with their corresponding reference images consumed approximately identical to **REFERENCE**.

Table 2 presents the statistical summary across all evaluation prompts. The upper half shows that **OURS** and **UNIFORM** achieve significantly higher efficiency than **REFERENCE**. Compared with alternative methods in the lower half, **OURS** also exhibits superior performance. These results evidence the effectiveness of our method in achieving more quality-computation-balanced optimization for image generation diffusion models.

**Overall quality gain** The previous analysis suggests that **OURS** and **UNIFORM** seem to exhibit comparable efficiency per step, and it may not be immediately clear that our technique is better than selecting a constant number of steps, as with the **UNIFORM** condition. Note that **OURS** and **UNIFORM** share the same total number of denoising steps; we further measure their relative quality as the ratio between the two,

$$\frac{m_{t_{\text{OURS}}}(p)}{m_{t_{\text{UNIFORM}}}(p)} - 1. \quad (9)$$

Here,  $t_{\text{OURS}}$  and  $t_{\text{UNIFORM}}$  indicate the timestep numbers suggested by **OURS** and **UNIFORM**, respectively. Intuitively, the positive or negative ratio values indicate how much **OURS** outperforms or underperforms than **UNIFORM**. Figure 8a visualizes the results after computing av-

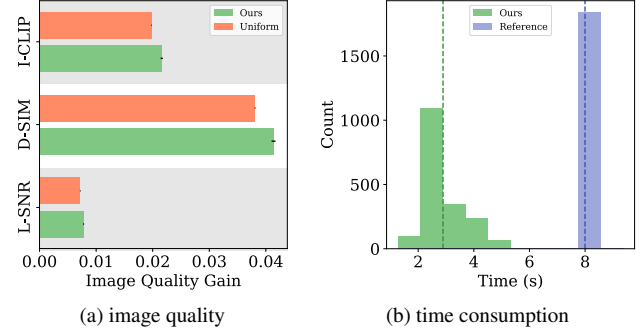


Figure 8. *Quantitative results.* (a) We plot the average image quality gain, defined in Equation (8), of conditions **OURS** and **UNIFORM** for the three perceptual metrics. (b) Average computation time (in seconds) with the corresponding number of forward denoising steps of conditions **OURS** and **REFERENCE**.

erage relative quality over all images in the test set. This results in relative quality of  $6.6\% \pm 0.8\%$  for  $m=\text{L-SNR}$ ,  $8.4\% \pm 0.9\%$  for  $m=\text{D-SIM}$ , and  $8.7\% \pm 0.9\%$  for  $m=\text{I-CLIP}$ . These results show that, despite having the same total number of denoising timesteps (i.e., same total computation), **OURS** exhibits significant quality gain over **UNIFORM**. This is also evidenced by our subjective study in the following Section 4.4.

**Time consumption** To measure the tangible benefits between **REFERENCE** and **OURS**, we measure their time consumption as seconds per image (SPI) on an NVIDIA RTX 3090 GPU. As shown in Figure 8b, with the entire evaluation dataset, **OURS** achieved  $2.89 \pm 0.87$  SPI versus **REFERENCE** at  $8.00 \pm 0.039$  SPI, which is 63.9% of the time of **REFERENCE**, indicating significantly reduced computational resource usage.

### 4.3. Image Quality and Diversity

We also compute the inception score (IS) to measure the generated image quality and diversity of the three conditions. The IS scores of **OURS**, **UNIFORM**, and **REFERENCE** were 27.9, 27.9, and 28.7, respectively, which demonstrates that BudgetFusion achieves computation savings without substantially compromising image quality and diversity. Furthermore, we include visual results of our method in the Supplementary Materials.

### 4.4. Subjective Crowdsourcing Study

As visualized in the insets of Section 4.4, we conducted a crowd-sourced user study with 72 participants through the platform *Prolific* to determine whether images generated with our technique are of high quality. Mantiuk et al. [34] found that forced-choice studies require fewer trials, reduce variance in results, and provide an unambiguous task



for participants. As such, we ran a two-alternative forced-choice (2AFC) study to measure participants’ preference for images generated by **OURS** and **UNIFORM**. During each trial, participants were presented with the reference and two test images, one generated by either **OURS** or **UNIFORM**. Users were instructed to select the image with higher image quality, with respect to **REFERENCE**. In total, participants completed 100 trials, with prompts randomly sampled from the dataset described in Sec. 3.1. An additional 2AFC study was conducted on 78 participants to compare the quality between **REFERENCE** and **OURS**. Our study was approved by an Institutional Review Board (IRB).

**Results and discussion** The results are visualized in Section 4.4 as a distribution of percentage selection of **OURS**. Here, we define percentage selection as the proportion of trials in which users selected **OURS** over **UNIFORM** or **REFERENCE** (depending on the study task). The mean percentage of selection of **OURS** was  $60.3 \pm 3.9\%$ . In the study in which users compare **OURS** and **REFERENCE**, participants selected **OURS**  $35.2 \pm 8.4\%$  of the time, lower than 25% selection which is commonly used to define the 1 Just-Noticeable-Difference (1 JND) threshold in psychophysical studies. The 1 JND range is commonly used in prior literature attempting to determine perceptually unnoticeable threshold [9]. These results evidence that our BudgetFusion-guided diffusion model achieves significant computation savings without sacrificing subjectively perceived quality. It may be interesting, in future work, to determine a mapping from plateau computation (e.g., defined in Sec. 3.4) to percentage preference. We expand on this discussion in the next section.

## 5. Limitations and Future Work

**Sparsely sampled diffusion timesteps** While preparing the dataset in Section 3.1, we sample the timesteps  $T$  in a non-uniform fashion considering the perceptual power law and then linearly interpolate the perceptual metrics among them during model training (Section 3.3). This is due to the storage and computation efficiency. As a future follow-up, evaluating perceptual quality with dense and uniform sampling may provide more fine-grained guidance.

**Variable savings.** In this work, we develop an algorithm to compute the plateau point of three metrics (see Sec. 3.4), which is used to determine a dataset for driving our technique. Ultimately, optimal timesteps determined by **OURS** depends on this dataset. It may be useful to determine how this dataset could be modified, for example in order to select optimal timesteps which require a pre-defined amount of compute.

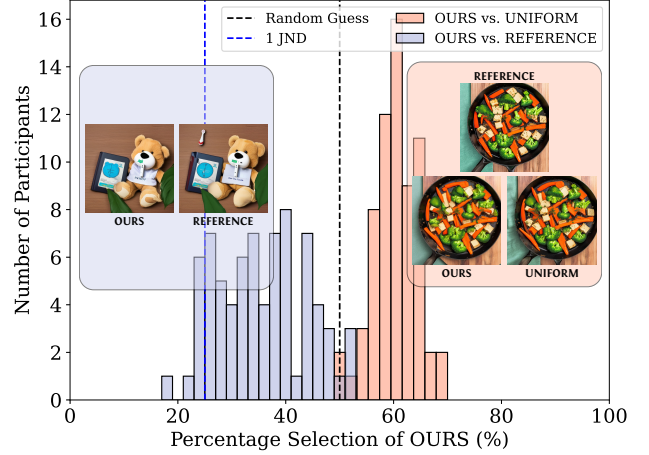


Figure 9. *Crowdsourced user study results.* Here (top) we visualize user study results, with percentage selection on the  $x$ -axis and number of participants on the  $y$ -axis. The green distribution are results for the **OURS** vs. **UNIFORM** study, and the violet distribution is that of **OURS** vs. **REFERENCE**. Random guess (50%) is visualized as the black dashed line, and 1 JND threshold is the blue dashed line. The insets show examples of presented stimuli to users for each study.

**Extension to videos.** BudgetFusion focuses on optimizing the quality-computation efficiency for image generation. More recently, significant advancements have been made to high-fidelity video generation [5, 12, 15]. Accessing the perceptual quality in the spatio-temporal domain would require a substantial amount of data and perceptual measurements [4, 35], and therefore beyond the scope of this research as the first attempt to guide diffusion models by human visual perception. As an exciting future direction, we envision solutions such as latent feature extraction [55] may shed light on reducing the required data volume for robust guidance.

## 6. Conclusion

In this paper, we present BudgetFusion, a predictive perceptual guidance for diffusion models. Given a text prompt, it suggests the most efficient timesteps *before* the computationally intensive neural-network-based denoising diffusion starts. That is, it guides the diffusion toward optimized “perceptual gain per step”. Our objective analysis and user studies show that this is achieved without compromising perceptual quality and content diversity. As “*making an image with generative AI uses as much energy as charging your phone*” [36], we hope this research will pave the way for future human-centered approaches to address the surging questions of how to optimize the computational and emission costs of generative models.

## References

- [1] Manuele Barraco, Marcella Cornia, Silvia Cascianelli, Lorenzo Baraldi, and Rita Cucchiara. The unreasonable effectiveness of clip features for image captioning: an experimental analysis. In *proceedings of the IEEE/CVF conference on computer vision and pattern recognition*, pages 4662–4670, 2022. 4
- [2] Yu-Hui Chen, Raman Sarokin, Juhyun Lee, Jiuqiang Tang, Chuo-Ling Chang, Andrei Kulik, and Matthias Grundmann. Speed is all you need: On-device acceleration of large diffusion models via gpu-aware optimizations. In *Proceedings of the IEEE/CVF Conference on Computer Vision and Pattern Recognition*, pages 4650–4654, 2023. 2
- [3] Mohamed Amine Cheragui, Abdelhalim Hafedh Dahou, and Amin Abdedaïem. Exploring bert models for part-of-speech tagging in the algerian dialect: A comprehensive study. In *Proceedings of the 6th International Conference on Natural Language and Speech Processing (ICNLSP 2023)*, pages 140–150, 2023. 5
- [4] Shyamprasad Chikkerur, Vijay Sundaram, Martin Reisslein, and Lina J Karam. Objective video quality assessment methods: A classification, review, and performance comparison. *IEEE transactions on broadcasting*, 57(2):165–182, 2011. 8
- [5] Florinel-Alin Croitoru, Vlad Hondru, Radu Tudor Ionescu, and Mubarak Shah. Diffusion models in vision: A survey. *IEEE Transactions on Pattern Analysis and Machine Intelligence*, 2023. 8
- [6] Steffen Czolbe, Oswin Krause, Ingemar Cox, and Christian Igel. A loss function for generative neural networks based on watson’s perceptual model. *Advances in Neural Information Processing Systems*, 33:2051–2061, 2020. 3
- [7] Scott J Daly. Visible differences predictor: an algorithm for the assessment of image fidelity. In *Human Vision, Visual Processing, and Digital Display III*, pages 2–15. SPIE, 1992. 2
- [8] Ralf Engbert and Konstantin Mergenthaler. Microsaccades are triggered by low retinal image slip. *Proceedings of the National Academy of Sciences*, 103(18):7192–7197, 2006. 5
- [9] Stephanie Fu, Netanel Tamir, Shobhita Sundaram, Lucy Chai, Richard Zhang, Tali Dekel, and Phillip Isola. Dreamsim: Learning new dimensions of human visual similarity using synthetic data. *Advances in Neural Information Processing Systems*, 36, 2024. 2, 4, 8
- [10] Alex Graves and Jürgen Schmidhuber. Framewise phoneme classification with bidirectional lstm and other neural network architectures. *Neural networks*, 18(5-6):602–610, 2005. 5
- [11] Alex Graves, Abdel-rahman Mohamed, and Geoffrey Hinton. Speech recognition with deep recurrent neural networks. In *2013 IEEE international conference on acoustics, speech and signal processing*, pages 6645–6649. Ieee, 2013. 2
- [12] Yuwei Guo, Ceyuan Yang, Anyi Rao, Yaohui Wang, Yu Qiao, Dahua Lin, and Bo Dai. Animatediff: Animate your personalized text-to-image diffusion models without specific tuning. *arXiv preprint arXiv:2307.04725*, 2023. 8
- [13] Geoffrey E Hinton, Nitish Srivastava, Alex Krizhevsky, Ilya Sutskever, and Ruslan R Salakhutdinov. Improving neural networks by preventing co-adaptation of feature detectors. *arXiv preprint arXiv:1207.0580*, 2012. 5
- [14] Jonathan Ho, Ajay Jain, and Pieter Abbeel. Denoising diffusion probabilistic models. *Advances in neural information processing systems*, 33:6840–6851, 2020. 1, 2
- [15] Jonathan Ho, Tim Salimans, Alexey Gritsenko, William Chan, Mohammad Norouzi, and David J Fleet. Video diffusion models. *Advances in Neural Information Processing Systems*, 35:8633–8646, 2022. 8
- [16] Akshay Jindal, Krzysztof Wolski, Karol Myszkowski, and Rafał K Mantiuk. Perceptual model for adaptive local shading and refresh rate. *ACM Transactions on Graphics (TOG)*, 40(6):1–18, 2021. 3
- [17] Justin Johnson, Alexandre Alahi, and Li Fei-Fei. Perceptual losses for real-time style transfer and super-resolution. In *Computer Vision—ECCV 2016: 14th European Conference, Amsterdam, The Netherlands, October 11–14, 2016, Proceedings, Part II 14*, pages 694–711. Springer, 2016. 3
- [18] Lynn H Kaack, Priya L Donti, Emma Strubell, George Kamiya, Felix Creutzig, and David Rolnick. Aligning artificial intelligence with climate change mitigation. *Nature Climate Change*, 12(6):518–527, 2022. 1
- [19] Tero Karras, Miika Aittala, Timo Aila, and Samuli Laine. Elucidating the design space of diffusion-based generative models. *Advances in Neural Information Processing Systems*, 35:26565–26577, 2022. 2, 3
- [20] Kate Crawford. Generative ai’s environmental costs are soaring — and mostly secret. *Nature World View*, 2024. 1
- [21] Peter Kellman and Elliot R McVeigh. Image reconstruction in snr units: a general method for snr measurement. *Magnetic resonance in medicine*, 54(6):1439–1447, 2005. 4
- [22] Jacob Devlin Ming-Wei Chang Kenton and Lee Kristina Toutanova. Bert: Pre-training of deep bidirectional transformers for language understanding. In *Proceedings of NAACL-HLT*, pages 4171–4186, 2019. 5
- [23] Lijiang Li, Huixia Li, Xiwu Zheng, Jie Wu, Xuefeng Xiao, Rui Wang, Min Zheng, Xin Pan, Fei Chao, and Rongrong Ji. Autodiffusion: Training-free optimization of time steps and architectures for automated diffusion model acceleration. In *Proceedings of the IEEE/CVF International Conference on Computer Vision*, pages 7105–7114, 2023. 1, 2
- [24] Muyang Li, Tianle Cai, Jiaxin Cao, Qingsheng Zhang, Han Cai, Junjie Bai, Yangqing Jia, Kai Li, and Song Han. Distri-fusion: Distributed parallel inference for high-resolution diffusion models. In *Proceedings of the IEEE/CVF Conference on Computer Vision and Pattern Recognition*, pages 7183–7193, 2024. 7
- [25] Yanyu Li, Huan Wang, Qing Jin, Ju Hu, Pavlo Chemerys, Yun Fu, Yanzhi Wang, Sergey Tulyakov, and Jian Ren. Snapfusion: Text-to-image diffusion model on mobile devices within two seconds. *Advances in Neural Information Processing Systems*, 36, 2024. 1, 2
- [26] Tsung-Yi Lin, Michael Maire, Serge Belongie, James Hays, Pietro Perona, Deva Ramanan, Piotr Dollár, and C Lawrence Zitnick. Microsoft coco: Common objects in context. In *Computer Vision—ECCV 2014: 13th European Conference, Zurich, Switzerland, September 6–12, 2014, Proceedings, Part V 13*, pages 740–755. Springer, 2014. 3, 4

- [27] Luping Liu, Yi Ren, Zhijie Lin, and Zhou Zhao. Pseudo numerical methods for diffusion models on manifolds. *arXiv preprint arXiv:2202.09778*, 2022. 2
- [28] Xingchao Liu, Xiwen Zhang, Jianzhu Ma, Jian Peng, et al. InstafLOW: One step is enough for high-quality diffusion-based text-to-image generation. In *The Twelfth International Conference on Learning Representations*, 2023. 1, 2
- [29] Cheng Lu, Yuhao Zhou, Fan Bao, Jianfei Chen, Chongxuan Li, and Jun Zhu. Dpm-solver: A fast ode solver for diffusion probabilistic model sampling in around 10 steps. *Advances in Neural Information Processing Systems*, 35:5775–5787, 2022. 2
- [30] Simian Luo, Yiqin Tan, Longbo Huang, Jian Li, and Hang Zhao. Latent consistency models: Synthesizing high-resolution images with few-step inference. *arXiv preprint arXiv:2310.04378*, 2023. 2
- [31] Xinyin Ma, Gongfan Fang, and Xinchao Wang. Deepcache: Accelerating diffusion models for free. In *The IEEE/CVF Conference on Computer Vision and Pattern Recognition*, 2024. 7
- [32] UB Mahadevaswamy and P Swathi. Sentiment analysis using bidirectional lstm network. *Procedia Computer Science*, 218:45–56, 2023. 5
- [33] Rafał Mantiuk, Kil Joong Kim, Allan G Rempel, and Wolfgang Heidrich. Hdr-vdp-2: A calibrated visual metric for visibility and quality predictions in all luminance conditions. *ACM Transactions on graphics (TOG)*, 30(4):1–14, 2011. 2
- [34] Rafał K Mantiuk, Anna Tomaszewska, and Radosław Mantiuk. Comparison of four subjective methods for image quality assessment. In *Computer graphics forum*, pages 2478–2491. Wiley Online Library, 2012. 7
- [35] Rafał K Mantiuk, Gyorgy Denes, Alexandre Chapiro, Anton Kaplanyan, Gizem Rufo, Romain Bachy, Trisha Lian, and Anjul Patney. Fovvideovdp: A visible difference predictor for wide field-of-view video. *ACM Transactions on Graphics (TOG)*, 40(4):1–19, 2021. 2, 8
- [36] Melissa Heikkilä. Making an image with generative ai uses as much energy as charging your phone. *MIT Technology Review*, 2023. 8
- [37] Chenlin Meng, Robin Rombach, Ruiqi Gao, Diederik Kingma, Stefano Ermon, Jonathan Ho, and Tim Salimans. On distillation of guided diffusion models. In *Proceedings of the IEEE/CVF Conference on Computer Vision and Pattern Recognition*, pages 14297–14306, 2023. 1, 2
- [38] Nasir Mohammad Khalid, Tianhao Xie, Eugene Belilovsky, and Tiberiu Popa. Clip-mesh: Generating textured meshes from text using pretrained image-text models. In *SIGGRAPH Asia 2022 conference papers*, pages 1–8, 2022. 4
- [39] Viet Nguyen, Giang Vu, Tung Nguyen Thanh, Khoat Than, and Toan Tran. On inference stability for diffusion models. In *Proceedings of the AAAI Conference on Artificial Intelligence*, pages 14449–14456, 2024. 3
- [40] Alexander Quinn Nichol and Prafulla Dhariwal. Improved denoising diffusion probabilistic models. In *International conference on machine learning*, pages 8162–8171. PMLR, 2021. 2
- [41] Italo Lopes Oliveira, Diego Moussallem, Luís Paulo Faina Garcia, and Renato Fileto. Optic: A deep neural network approach for entity linking using word and knowledge embeddings. In *ICEIS (I)*, pages 315–326, 2020. 5
- [42] Sylvain Paris, Samuel W Hasinoff, and Jan Kautz. Local laplacian filters: Edge-aware image processing with a laplacian pyramid. *ACM Trans. Graph.*, 30(4):68, 2011. 4
- [43] Anjul Patney, Marco Salvi, Joohwan Kim, Anton Kaplanyan, Chris Wyman, Nir Benty, David Luebke, and Aaron Lefohn. Towards foveated rendering for gaze-tracked virtual reality. *ACM Transactions on Graphics (TOG)*, 35(6):1–12, 2016. 3
- [44] Konpat Preechakul, Nattanat Chatthee, Suttisak Widadwongsa, and Supasorn Suwajanakorn. Diffusion autoencoders: Toward a meaningful and decodable representation. In *Proceedings of the IEEE/CVF Conference on Computer Vision and Pattern Recognition*, pages 10619–10629, 2022. 2
- [45] Alec Radford, Jong Wook Kim, Chris Hallacy, Aditya Ramesh, Gabriel Goh, Sandhini Agarwal, Girish Sastry, Amanda Askell, Pamela Mishkin, Jack Clark, et al. Learning transferable visual models from natural language supervision. In *International conference on machine learning*, pages 8748–8763. PMLR, 2021. 3, 4
- [46] Aditya Ramesh, Mikhail Pavlov, Gabriel Goh, Scott Gray, Chelsea Voss, Alec Radford, Mark Chen, and Ilya Sutskever. Zero-shot text-to-image generation. In *International conference on machine learning*, pages 8821–8831. Pmlr, 2021. 2
- [47] Robin Rombach, Andreas Blattmann, Dominik Lorenz, Patrick Esser, and Björn Ommer. High-resolution image synthesis with latent diffusion models. In *Proceedings of the IEEE/CVF conference on computer vision and pattern recognition*, pages 10684–10695, 2022. 1, 2, 3, 4
- [48] Tim Salimans and Jonathan Ho. Progressive distillation for fast sampling of diffusion models. *arXiv preprint arXiv:2202.00512*, 2022. 1, 2
- [49] Sarah Wells. Generative ai’s energy problem today is foundational. *IEEE Spectrum*, 2023. 1
- [50] Axel Sauer, Frederic Boesel, Tim Dockhorn, Andreas Blattmann, Patrick Esser, and Robin Rombach. Fast high-resolution image synthesis with latent adversarial diffusion distillation. *arXiv preprint arXiv:2403.12015*, 2024. 1, 2
- [51] Sima Siami-Namini, Neda Tavakoli, and Akbar Siami Namin. The performance of lstm and bilstm in forecasting time series. In *2019 IEEE International conference on big data (Big Data)*, pages 3285–3292. IEEE, 2019. 5
- [52] Jiaming Song, Chenlin Meng, and Stefano Ermon. Denoising diffusion implicit models. *arXiv preprint arXiv:2010.02502*, 2020. 2, 7
- [53] Yang Song, Prafulla Dhariwal, Mark Chen, and Ilya Sutskever. Consistency models. *arXiv preprint arXiv:2303.01469*, 2023. 2
- [54] Frederico Dias Souza and João Baptista de Oliveira e Souza Filho. Bert for sentiment analysis: pre-trained and fine-tuned alternatives. In *International Conference on Computational Processing of the Portuguese Language*, pages 209–218. Springer, 2022. 5
- [55] Guanxiong Sun, Chi Wang, Zhaoyu Zhang, Jiankang Deng, Stefanos Zafeiriou, and Yang Hua. Spatio-temporal prompting network for robust video feature extraction. In *Proceed-*



- ings of the IEEE/CVF International Conference on Computer Vision*, pages 13587–13597, 2023. [8](#)
- [56] Zhou Wang, Alan C Bovik, Hamid R Sheikh, and Eero P Simoncelli. Image quality assessment: from error visibility to structural similarity. *IEEE transactions on image processing*, 13(4):600–612, 2004. [2](#)
  - [57] Zihao Wang, Wei Liu, Qian He, Xinglong Wu, and Zili Yi. Clip-gen: Language-free training of a text-to-image generator with clip. *arXiv preprint arXiv:2203.00386*, 2022. [4](#)
  - [58] Yongqi Yang, Ruoyu Wang, Zhihao Qian, Ye Zhu, and Yu Wu. Diffusion in diffusion: Cyclic one-way diffusion for text-vision-conditioned generation. *arXiv preprint arXiv:2306.08247*, 2023. [4](#)
  - [59] Tongtong Yuan, Weihong Deng, Jian Tang, Yinan Tang, and Binghui Chen. Signal-to-noise ratio: A robust distance metric for deep metric learning. In *Proceedings of the IEEE/CVF conference on computer vision and pattern recognition*, pages 4815–4824, 2019. [4](#)
  - [60] Richard Zhang, Phillip Isola, Alexei A Efros, Eli Shechtman, and Oliver Wang. The unreasonable effectiveness of deep features as a perceptual metric. In *Proceedings of the IEEE conference on computer vision and pattern recognition*, pages 586–595, 2018. [2](#)

# BudgetFusion: Perceptually-Guided Adaptive Diffusion Models

## Supplementary Material

### Additional Model Training Details

We used one A100 to train models, and 30 minutes for L-SNR and D-SIM models, and 60 minutes for the I-CLIP model. In inference, our model takes 0.004 seconds to predict quality scores for a given prompt.

### User Study Protocol

Figure 10 and 11 visualize our crowdsourced user study protocol as a time sequence and example stimuli.

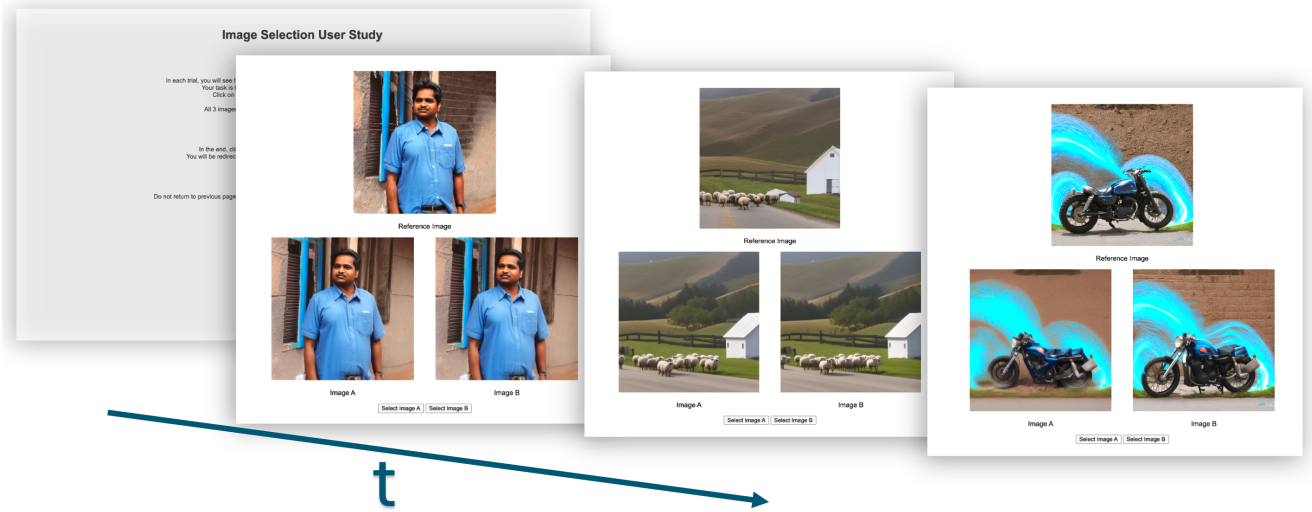


Figure 10. *User study protocol OURS vs. UNIFORM.* In each user study trial, the participant will see three images: a reference image in the middle, and 2 test images (Image A and Image B). The task is to select the image that is more similar to the reference image. The participant needs to click on the button below or press the keyboard to choose A/B.

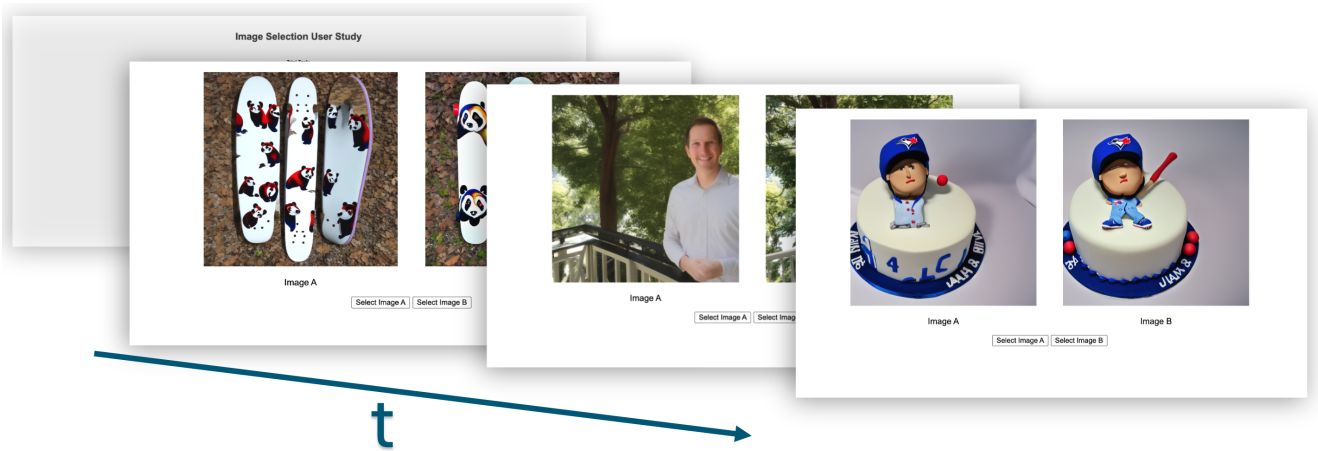
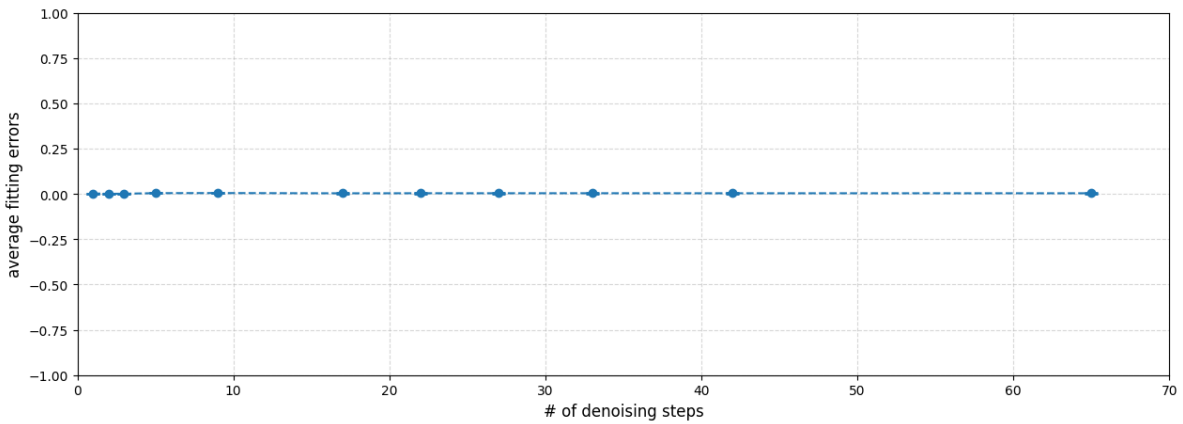


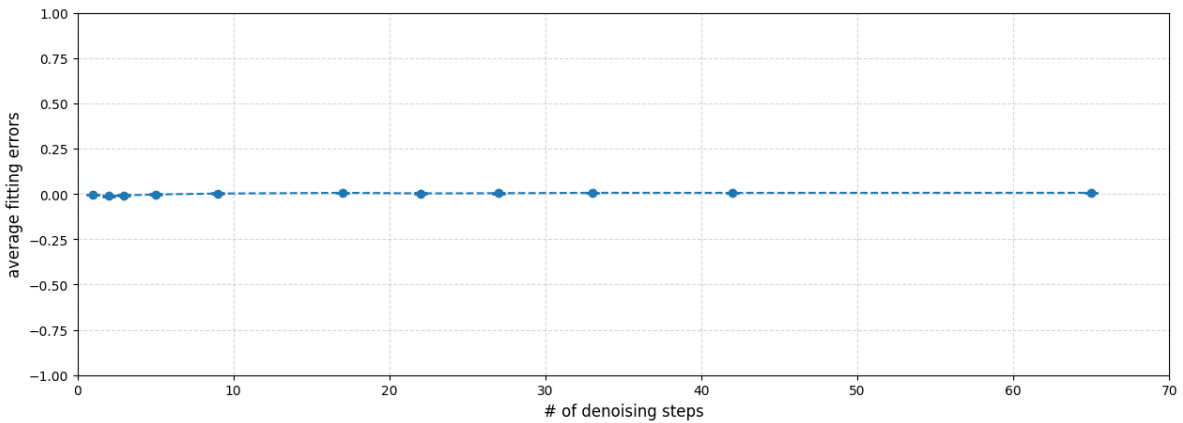
Figure 11. *User study protocol OURS vs. REFERENCE.* In each trial, the participant will see two images: Image A and Image B. One of these two images is the reference image, which is of higher quality. The participants need to choose the one they think is the reference image. They will click on the button below or press the keyboard to choose A/B.

## Visualization of Evaluation Errors

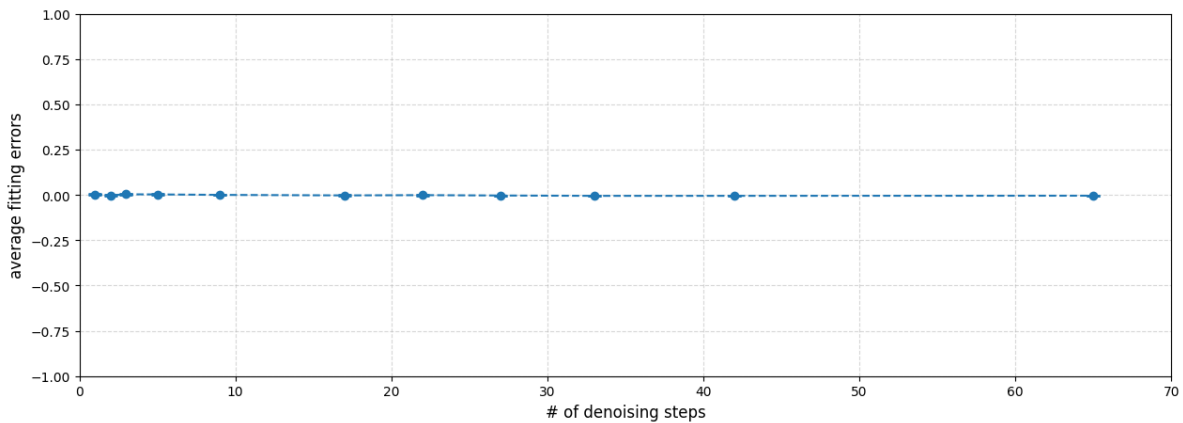
Figure 12 visualizes the fitting error of our LSTM model across all three perceptual metrics. For all number of denoising steps, error is low. This shows that our model is consistent across different number of timesteps.



(a) L-SNR error



(b) D-SIM error



(c) I-CLIP error

Figure 12. Visualizing fitting errors.  $x$ - and  $y$ -axis denotes the model-suggested number of denoising steps, and the corresponding fitting errors, respectively. The error bars indicate standard error. The results evidence the high accuracy and consistency of our LSTM prediction.



## Additional Qualitative Results

Figure 13 provides additional visual comparisons of BudgetFusion-generated images.



Figure 13. *Additional qualitative results.* We include qualitative results of a pre-trained diffusion model with images generated at increasing denoising timesteps. The center column represents optimal timestep,  $t^*$ , predicted with our technique, and with each row having increased  $t^*$ . The text prompts used to generate the images are in the left column, and the three scores used to compute the optimal timestep are in the right column. Green, blue and red curves correspond to metrics scores of L-SNR, D-SIM, and I-CLIP, respectively.